European Review for Medical and Pharmacological Sciences 2018; 22: 2334-2342

Stemness-related changes of CD133⁻ cells in nasopharyngeal carcinoma after x-ray radiation at the median lethal dose

W.-W. DAI, S. LIU, X.-J. LIU, Z.-P. PENG

Department of Radiological Medicine, College of Basic Medical, Chongqing Medical University, Chongqing, China

Weiwei Dai and Shuang Liu contributed equally to this work

Abstract. – OBJECTIVE: To investigate the effect of X-ray radiation at the median lethal dose (LD50) on the outcome of a cluster of differentiation 133 (CD133)⁻ cells in nasopharyngeal carcinoma.

MATERIALS AND METHODS: CD133⁻ cells were obtained from human nasopharyngeal carcinoma cells (CNE-1 and CNE-2) based on CD133-labeled fluorescence-activated cell sorting (FACS) and magnetic-activated cell sorting (MACS), respectively. Changes in invasion ability and *in-vivo* tumorigenicity of CD133- cells before and after X-ray radiation at LD50 were observed. Moreover, CD133, SRY-related HMG-box 2 (SOX2), and organic carnitine transporter 4 (OCT4) expression changes were detected by reverse transcription-polymerase chain reaction (RT-PCR) and Western blotting.

RESULTS: The invasion ability and *in-vivo* tumorigenicity of CD133⁺ cell subsets were significantly stronger than those of CD133⁻ cell subsets. After X-ray radiation at LD50, the invasion ability of CD133- cell subsets and *in-vivo* tumorigenicity were significantly increased. RT-PCR and Western blotting results manifested that the expression levels of CD133, SOX2, and OCT4 were remarkably up-regulated after radiation.

CONCLUSIONS: X-ray radiation at LD50 can enhance the stemness potential by up-regulating the expression of stemness-related genes in nasopharyngeal carcinoma CD133- cells.

Key Words

Nasopharyngeal carcinoma, Cancer stem cell, Radiation-induced radiotherapy resistance, CD133.

Introduction

Radiotherapy has made significant contributions to cancer therapy. However, despite of continuous improvements, tumor recurrence and radioresistance still occur in a high proportion of patients. An underlying reason for this radioresistance might be attributable to the presence of cancer stem cells (CSCs). Hierarchically organized tumors have added a new level of complexity to therapy failure. CSCs are the root of cancers and resist chemotherapy and radiotherapy, which lead to cancer recurrence even many years after therapy. Since the CSC hypothesis was proposed, a large number of experiments have demonstrated that CSCs objectively exist, and they can be isolated from a variety of primary tumor tissues and cell lines[1,2]. It is generally accepted that CSCs are a kind of cell with stem cell characteristics, which have a high proliferative capacity and a multidirectional differentiation potential[3]. CSCs are the root of tumor recurrence and metastasis, and the direct killing or eradication of them is the focus and the leading edge of cancer therapy research[4]. On the other hand, if the origin of CSCs can be testified, suppressing CSCs from their roots will be quite valuable in the application.

At present, there are two views on the origin of CSC: 1) due to the stagnation and blockage of stem cell differentiation in normal tissues, cells lose normal regulation ability and stagnate at certain stages of differentiation to indefinitely proliferate, thus forming CSCs[5]; 2) committed progenitors or differentiated cells in normal tissues mutate and regain CSC characteristics, thus transforming into CSCs[6]. However, there is still no accepted theory and reliable experimental basis to confirm the origin of CSCs. Cluster of differentiation 133 $(CD133)^+$ and $CD133^-$ cells are obtained by separating nasopharyngeal carcinoma cell lines via immunomagnetic beads and fluorescence-activated cell sorting (FACS). $CD133^+$ and $CD133^-$ cells are considered to be CSCs and cancer cells[7]. In the course of 4 Gy X-ray radiation, it was demonstrated that the

Corresponding Author: Zhiping Peng, MD; e-mail: pengzhiping@cqmu.edu.cn

invasion ability of CD133⁻, tumorigenesis speed, and expression of proteins associated with stem cells were markedly enhanced, suggesting that CSCs may be transformed from cancer cells.

We investigated the effect of X-ray radiation at the median lethal dose (LD50) on the outcome of cluster of differentiation 133 (CD133)⁻ cells in nasopharyngeal carcinoma.

Materials and Methods

Cell Culture

Human nasopharyngeal carcinoma cells (CNE-1 and CNE-2) were routinely cultured (37°C, 5% CO_2) in Roswell Park Memorial Institute-1640 (RPMI-1640) (Invitrogen, Carlsbad, CA, USA) medium containing 10% fetal bovine serum (FBS, Gibco, Rockville, MD, USA), 100 U/mL penicillin and 50 μg/mL streptomycin (Jiangsu Changjiang Pharmaceutical Co., Yancheng, China), and they underwent passage once every 2-3 days.

CD133 Cell Sorting

According to the operating instructions of magnetic-activated cell sorting (MACS), the separation by magnetic beads was conducted for 10^8 CNE-1 cells in the logarithmic growth phase. CNE-1 cells were added with buffer for washing, centrifuged (300 g, 10 min) and resuspended in 300 μL buffer. After that, 100 μL blocking agents and 300 μL CD133 immunomagnetic beads were added and mixed well, and then they were placed in a refrigerator at 4°C away from light. Afterwards, 1,000 μL buffer was added for washing, and cells were centrifuged (300 g, 10 min) and resuspended in 500 μL buffer. According to the operating instructions, the sorting rack, sorter, filter candle and filter were placed and rinsed with 500 μL buffer. The resuspended CNE-1 cells passed through the filter candle, followed by collection of $CD133^-$ and $CD133^+$ cells, respectively. $CD133^+$ cells were cultured in a serum-free medium [Dulbecco's modified Eagle's medium and Ham's F-12 nutrient mixture (DMEM/F12) containing 20 ng/mL basic fibroblast growth factor (bFGFs), 20 ng/mL epidermal growth factors (EGFs), 5% insulin and 0.4% bovine serum albumin (BSA)] (Gibco, Rockville, MD, USA), and $CD133^-$ cells were placed in a culture medium for further culture. All sorted cells were examined via FACS. The same operations were performed for CNE-2 cells.

Determination of the Median Lethal Dose (LD50) of Radiation

Cells in the culture flask were collected and counted. About 2,000 cells per well were seeded in a 96-well plate, and the amount of liquid in each well was made up to 200 μL. The 96-well plate was gently shaken to promote the even distribution of cells in the well. Next, cells were put into a cell incubator for 24 h. The 96-well plate was removed and sealed with the sealing glue. The cells were let stand for 20 min and placed under an X-ray machine for radiation. X-ray radiation parameters: 6MV-X, radiation field: 10 cm×10 cm, source-to-skin distance (SSD): 100 cm, dose rate: 0.2 Gy/min, and rack rotation angle: 180°. Cells were divided into sham radiation group (0 Gy), 2 Gy group, 4 Gy group, 6 Gy group and 8 Gy group. Each group was set with 3 repeated wells. At the end of the radiation, the culture was continued for 48 h. 3-(4,5-dimethylthiazolyl-2)-2,5-diphenyltetrazolium bromide (MTT) assay (Beyotime, Shanghai, China) was performed to measure the optical density values of groups with different radiation doses. The cell survival fraction-radiation dose curve was plotted, and LD50 was calculated.

Radiation Treatment

$CD133^-$ cells were collected from CNE-1 and CNE-2 cells, respectively, resuspended in 500 μLbuffer at 4°C and irradiated with X-rays at a radiation dose rate of 0.2 Gy/min for 20 min to collect cells for standby application.

Invasion Assay

$CD133^+$ cells extracted from CNE-1 cells and $CD133^-$ cells before and after radiation were collected, respectively, and 3×10^3 cells were seeded in the upper transwell chamber (Corning, NY, USA). In the lower chamber, 500 μL medium containing 20% fetal bovine serum (FBS) were added as a chemotaxis agent. After 24 h of routine culture and staining with crystal violet, the filter membrane was removed, and cells in the lower surface of the membrane were counted using an optical microscope. Five fields were randomly taken, and the mean value was calculated. Invasion ability = the number of invaded cells/the number of inoculated cells × 100%.

Real-Time Quantitative Polymerase Chain Reaction (RT-qPCR)

$CD133^+$ cells extracted from CNE-1 cells and $CD133^-$ cells before and after radiation were collected, followed by washing twice with buffer.

The total ribonucleic acid (RNA) was extracted according to TRIzol operating instructions (Invitrogen, Carlsbad, CA, USA). 1 μg total RNA was taken and reversely transcribed into complementary deoxyribonucleic acid (cDNA) using Reverse Transcription (RT) Enzyme Mix I (Thermo Fisher Scientific, Waltham, MA, USA), with 1 μL cDNA as a template for amplification and glyceraldehyde 3-phosphate dehydrogenase (GAPDH) as an internal reference (the internal reference and primer sequences were shown in Table I). Amplification conditions: pre-denaturation at 94°C for 90 s, denaturation at 94°C for 30 s, annealing at 55°C for 30 s, extension at 72°C for 60 s, 40 cycles, and 72°C for 5 min. The cycle threshold (Ct) value was analyzed using SLAN, and $2^{-\Delta\Delta Ct}$ method was applied to calculate the expression levels of CD133, SRY-related HMG-box 2 (SOX2), organic carnitine transporter 4 (OCT4) and Nanog mRNAs. The same operations were conducted in the CNE-2 cell group.

Western Blotting Assay

$CD133^+$ cells extracted from CNE-1 cells and proteins extracted from $CD133^-$ cells before and after radiation were collected for Western blotting experiments. The maker in a certain volume and each sample were added to the bottom of each well in turn. The upper-layer gel was applied for about 30 min with a voltage of 80 V, and the voltage was changed to 120 V when bromophenol blue entered the lower-layer gel under observation. About 1-1.5 h later, bromophenol blue was close to the bottom of the glass plate as observed, after which the electrophoresis was stopped. The protein bands isolated on the gel were transferred onto a polyvinylidene difluoride (PVDF, Millipore, Billerica, MA, USA) membrane via wet transfer electrophoresis (4°C, constant current) and sealed using 5% bovine serum albumin (BSA) for 2 h at room temperature. Primary antibodies were diluted in appropriate proportions, namely, β-actin (1:500), CD133 (1:1000), SOX2 (1:1000), OCT4 (1:1000) and Nanog (1:1000), and the PVDF membrane was placed into them at 4°C overnight. After that, the PVDF membrane was removed and placed on a plate, followed by washing with Tris-buffered saline and Tween 20 (TBST) for 3-4 times (5 min each). The secondary antibody was diluted to an appropriate concentration, with general dilution ratio of 1:5000. The membrane was placed in it and shaken slowly for 1 h at room temperature. Afterwards, the membrane was removed, placed on a plate on a shaker and washed with TBST for 4-5 times (15 min each). Finally, the membrane was exposed for film developing.

Table I. Primer sequences and products size for semi-quantitative RT-PCR.

Target gene	Primer sequences
SOX2	Forward: 5'-ATCAGCATGTATCTCCCCGG-3' Reverse: 5'-TACCGGGTTTTCTCCATGCT-3'
Nanog	Forward: 5'-TGAGTGTGGATCCAGCTTGT-3' Reverse: 5'-TCTCTGCAGAAGTGGGTTGT-3'
CD133	Forward: 5'-ACAGCGATCAAGGAGACCAA-3' Reverse: 5'-GTCAAGTTCTGCATCCACGG-3'
OCT4	Forward: 5'-GGTCCGAGTGTGGTTCTGTA-3' Reverse: 5'-CGAGGAGTACAGTGCAGTGA-3'
GAPDH	Forward: 5'-TGATTTGGTCGTATTGGGCG-3' Reverse: 5'-TGACGGTGCCATGGAATTTG-3'

Animal Model and Immunohistochemistry of Xenograft Tumors

$CD133^+$ cells extracted from CNE-1 cells and $CD133^-$ cells before and after radiation were separately collected and inoculated on the back of nude mice (10^2 cells, 3 nude mice in each group). 4 weeks later, the nude mice were sacrificed under the pentobarbital sodium anesthesia; the tumors were removed, and the tumor size was measured. The diameter of the tumors less than 5 mm was recorded as a failure to construct the transplanted tumor model. CD133 and OCT4 expression levels in tumors were analyzed using immunohistochemistry.

Statistical Analysis

Statistical Product and Service Solutions (SPSS) 19.0 software (Armonk, NY, USA) was adopted for statistical analysis. Measurement data were expressed as mean±standard deviation. Comparison between groups was done using One-way ANOVA test followed by Least Significant Difference (LSD). The univariate analysis was conducted for the intergroup comparison. $p<0.05$ represented that the difference was statistically significant.

Results

Cell Sorting

CD133 expression was measured via FACS. The results revealed that the expression rate of CD133 in CNE-1 cell line in the $CD133^+$ cell group was (96.13±1.79)% (recorded as CNE-1 $CD133^{high}$), and that in the $CD133^-$ cell group was (1.54%±0.84)% (recorded as CNE-1 $CD133^{low}$) ($p=0.0001$). Moreover, the expression rate of CD133 in CNE-2 cell

line in the CD133^{+} cell group was (98.02±0.71)% (recorded as CNE-2 CD133^{high}), and that in the CD133^{-} cell group was (1.34±0.25)% (recorded as CNE-2 CD133^{low}) (p=0.0001) (Figure 1A).

The results of Western blotting (Figure 1B-C) displayed that CD133 protein was expressed in all groups, but CD133 protein expression in CNE-1 CD133^{high} was markedly higher than that in CNE-1 CD133^{low} (p<0.05), and that in CNE-2 CD133^{high} was remarkably higher than that in CNE-2 CD133^{low} (p<0.05).

The results of Q-PCR (Figure 1D) manifested that CD133 mRNA was expressed in all groups, but CD133 mRNA expression in CNE-1 CD133^{high} was significantly higher than that in CNE-1 CD133^{low} (p<0.05), and that in CNE-2 CD133^{high} was significantly higher than that in CNE-2 CD133^{low} (p<0.05).

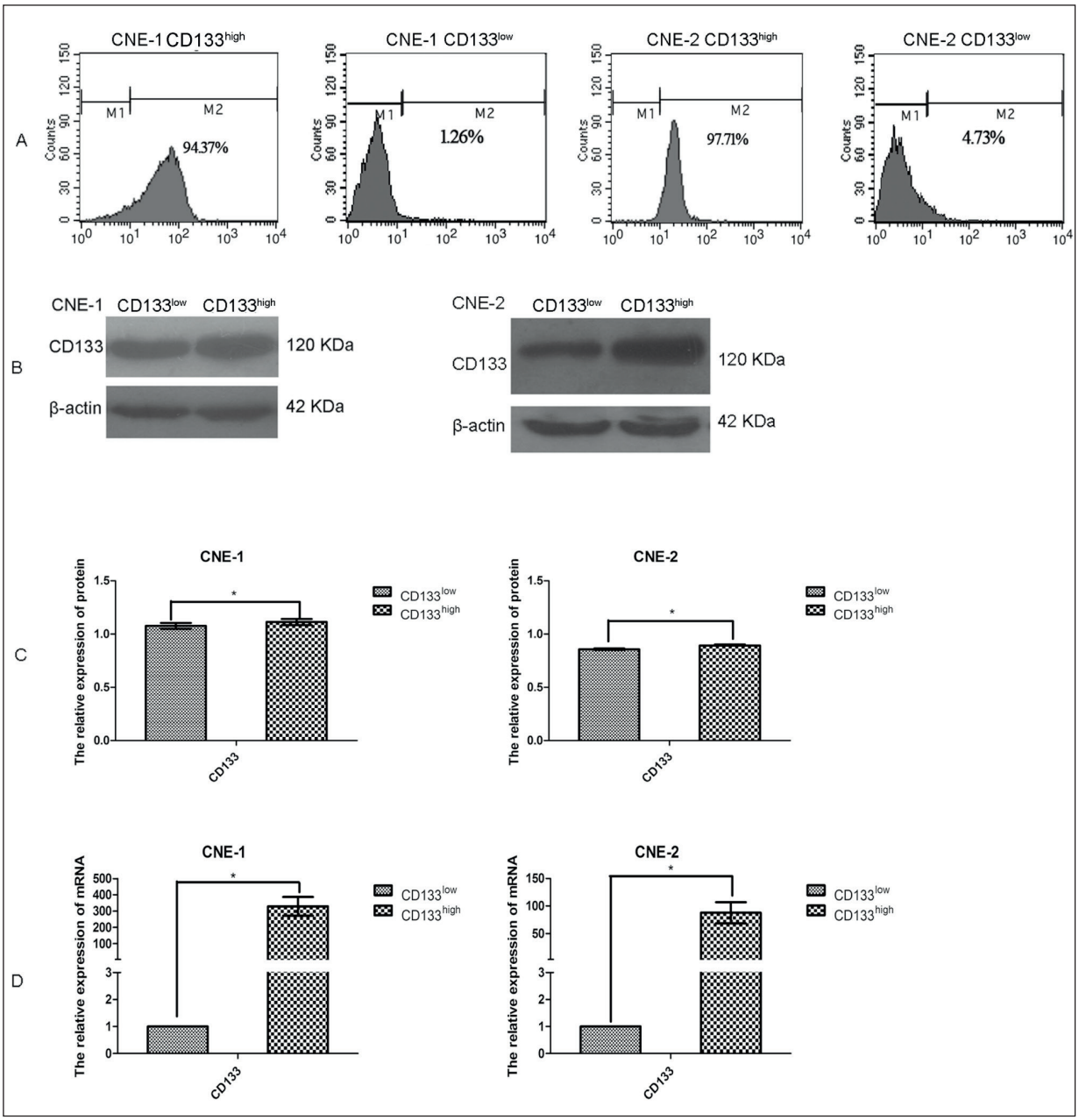

Figure 1. The difference between CD133^{+} and CD133^{-} cells (the expression level of CD133 in cancer cells *via* magnetic beads separation). **A**, CD133 expression is estimated by a standard FACS. **B-C**, Detection of the expressions of CD133 in CD133^{+} and CD133^{-} cells via Western blotting. **D**, CD133 mRNA expression.

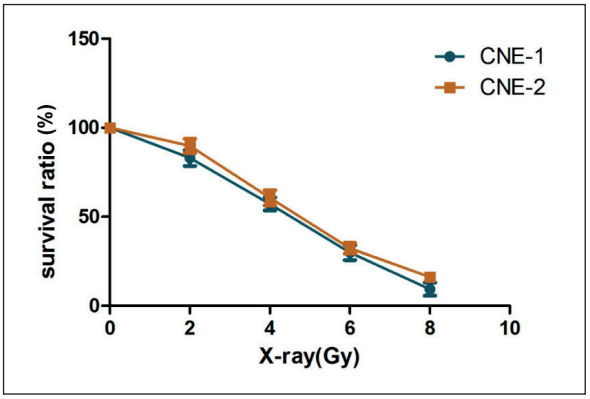

Figure 2. Survival fraction-radiation dose curve. CNE-1: LD50=4.439 Gy, CNE-2: LD50=4.821 Gy.

Screening of the Appropriate Dose of Radiation

MTT assay was employed to detect the inhibition of the growth of $CD133^-$ cells by radiation at different doses. LD50 of CNE-1 was 4.439 Gy, while that of CNE-2 was 4.821 Gy (Figure 2).

4 Gy X-Ray Radiation Enhanced $CD133^{low}$ Cell Invasion Ability

Ionizing radiation significantly enhanced the invasion ability of $CD133^-$ cells, but the invasion ability of $CD133^{-4Gy}$ cells [CNE-1: (16.2±1.71)%, CNE-2: (26.9±0.93)%] was far stronger than that of $CD133^-$ cells [CNE-1: (6.33±0.51)%, CNE-2: (6.01±0.45)%] ($p<0.01$) (Figure 3).

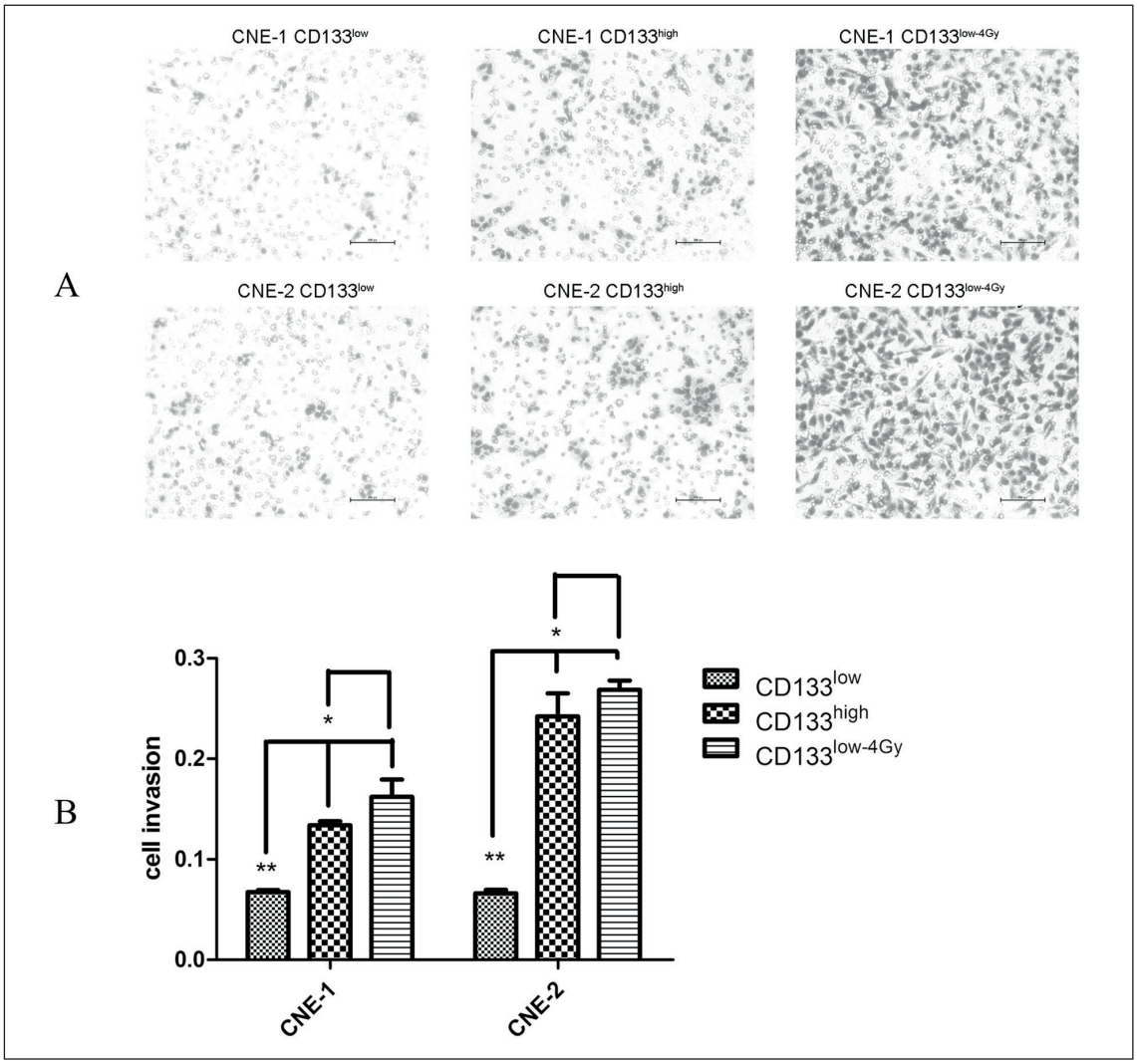

Figure 3. Detection of the invasion capacity of cells by a transwell assay. **A**, Cells under the microscope (200×). **B**, The histogram displays the migration of cells, indicating that the ratio of cells exposed to 4 Gy radiation is significantly increased compared with those of $CD133^-$ and $CD133^+$ cells. *$p<0.05$, **$p<0.01$.

Radiation Up-Regulated Stemness-Related Gene Expression

Significant increases in CD133, OCT4, SOX2 and Nanog mRNAs were detected inCNE-1 and CNE-2 CD133$^{-4\ Gy}$ cells. In consistence with the results of q-PCR, the expressions of OCT4, SOX2 and Nanog proteins in CD133^{-4Gy} cells were higher than those in CD133^{+} cells, and the expression of CD133 was also up-regulated to some extent. The analysis of CD133^{-4Gy} and CD133^{+} cells revealed that, although the expression of CD133 in the former was markedly higher than those in the latter, the expression levels of SOX2, OCT4, and Nanog in the latter were significantly higher (Figure 4).

Radiation-Promoted Tumorigenesis In Vivo

CD133^{+} and CD133^{-4Gy} tumors grew much faster than CD133^{-} tumors, and it was almost impossible to detect CD133^{-} tumors. At the same time, CD133^{-4Gy} tumors were larger than CD133^{+} tumors (Figure 5A-C), and hematoxylin and eosin (HE) staining of these tumors were showed in Figure 5D.

Immunohistochemical analysis confirmed significant increases in the expressions of CD133 and OCT4 in tumors (Figure 5E-F). These results indicated that 4 Gy X-ray radiation could enhance the *in-vivo* tumorigenicity of CNE-1 and CNE-2CD133^{-} cells.

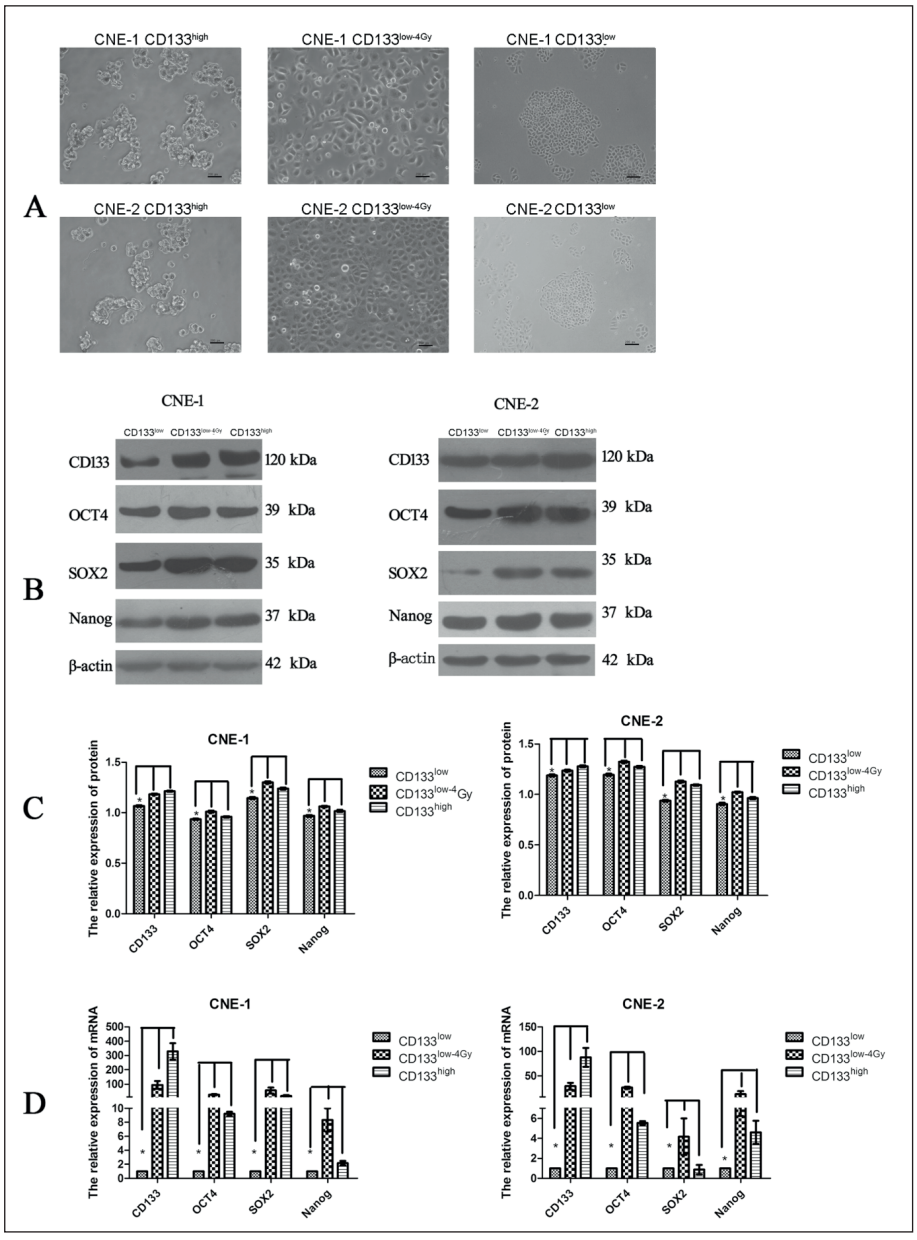

Figure 4. The expression of stemness-related genes is increased in CNE-1 and CNE-2 cells following radiation treatment. **A**, Morphology of the cells (200×). **B-C**, Western blotting results for CNE-1 and CNE-2 cells. **D**, Real-time q-PCR results for CNE-1 and CNE-2 cells. *p<0.05.

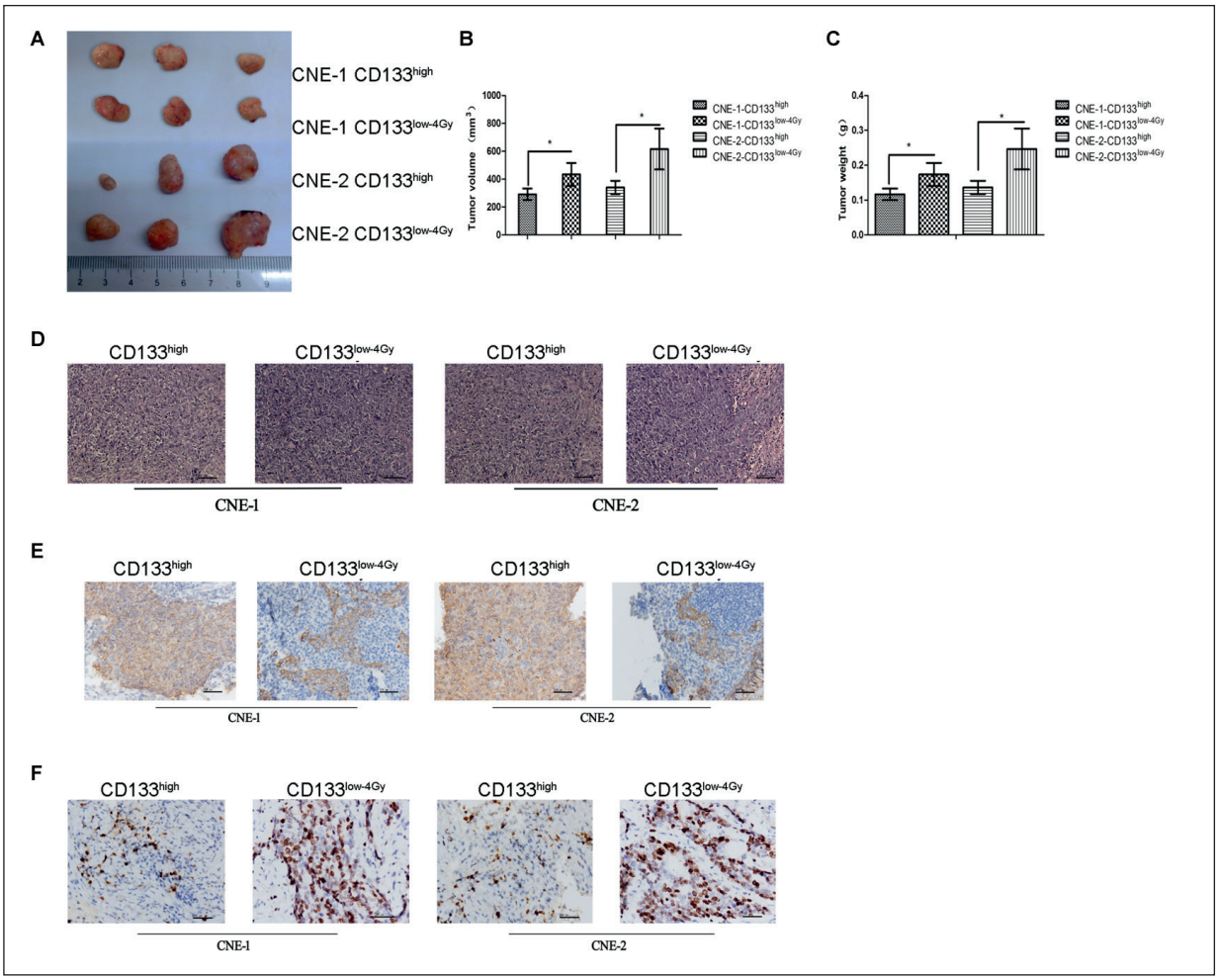

Figure 5. Radiation promotes tumorigenesis *in vivo*. The cells (5×102) are subcutaneously inoculated into the left flank of nude mice. The tumor size is measured weekly for four weeks. The ectopic tumor xenograft models using the $CD133^{+}$ and $CD133^{-4Gy}$ cells are successfully generated, but the $CD133^{-}$ cells fail to form tumors. **A**, Representative tumors generated from the $CD133^{+}$ and $CD133^{-4Gy}$ fractions from CNE-1 and CNE-2 cells. **B**-**C**, The tumor volume and weight, respectively. **D**, Hematoxylin and eosin (HE) staining of these tumors (400×). **E**, The expressions of CD133 in these tumor tissues (40×). **F**, The expressions of OCT4 in these tumor tissues (400×).*$p<0.05$.

Discussion

In this experiment, X-rays were applied to radiate the $CD133^{-}$ cell group, which demonstrated that the invasion ability of cells in this group was significantly increased and even higher than that in the $CD133^{+}$ cell group. Meanwhile, the expressions of OCT4, SOX2, and Nanogm RNAs and proteins in the radiated $CD133^{-}$ cell group obviously went up. OCT4, SOX2, and Nanog are key genes for human-induced pluripotent stem cell reprogramming[8,9], and their high expressions mean that the $CD133^{-}$ cells undergo stem cell-like transformation. CD133 is a special molecule on the surface of CSCs[10], and the expression of CD133 in radiated $CD133^{-}$ cells was still lower than that in $CD133^{+}$ cells. Additionally, a few (10^{2}) $CD133^{-}$, $CD133^{-4Gy}$ and $CD133^{+}$ cells were injected into 3 nude mice in *in-vitro* experiments. Tumors were not formed in the $CD133^{-}$ cell group, while they were formed *in vivo* in the $CD133^{-4Gy}$ and the $CD133^{+}$ cell group. Besides, the radiated $CD133^{-}$ cell group had a larger tumor volume than the $CD133^{+}$ cell group. These results indicated that X-ray radiation could enhance the stemness of $CD133^{-}$ cells.

CSCs are rare cells in tumor tissues, which have self-renewal and infinite multiplication ability as well as multi-directional differentiation potential. CSCs are also considered to be the root of tumor formation, development, invasion, and metastasis.

The constant differentiation of CSCs into cancer cells promotes tumorigenesis[11]. Therefore, exploring the origin of CSCs is of great significance for tumor prevention and treatment. In this work, CD133$^-$ nasopharyngeal carcinoma cells were radiated with 4 Gy X-rays, so as to observe changes in biological characteristics of cancer cells under external environmental stress. The results manifested that the invasion ability and tumorigenicity of radiated CD133$^-$ cells, as well as the expression of proteins associated with stem cells in them, were remarkably boosted, and they had CSC-like properties, suggesting that CSCs can be transformed from cancer cells.

In recent years, studies have confirmed the possibility of the transformation of cancer cells into CSCs. Lee et al[12] also induced the transformation of cancer cells into CSCs using tumor necrosis factor-alpha (TNF-α). In addition, Liang et al[13] also reported that the treatment of nasopharyngeal carcinoma and neuroblastoma with ultraviolet and mitomycin C can trigger a significant increase in CSCs. Bao et al[14] demonstrated that X-ray radiation can induce the increase in CD133$^+$ expression in glioma cells.

Our results showed that cancer cells possibly had the capacity to transform into CSCs. It was speculated that rays killed some cancer cells and also promoted the conversion of another part of cancer cells to CSCs. This partly explains the reason for the accelerated re-proliferation of cancer cells in the early stage of clinical radiotherapy with low-dose X-ray radiation[15], which also suggests that sufficient rays should be applied in tumor radiotherapy. These newly formed CSCs will form new tumors, which may be one of the reasons for tumor recurrence and metastasis. Meanwhile, these newly formed tumors have certain radiation resistance due to the experience of receiving radiation before, which reduces their sensitivity to the radiation at the original dose, resulting in a higher and higher radiation resistance of CSCs and the tumors they form. This suggests that the formation of CSCs should be prevented while cancer cells are killed during clinical radiotherapy.

The current experimental data revealed that ray radiation could improve the stemness of cancer cells, but the exact mechanism is not yet clear. At present, cancer cells can obtain stemness by three approaches: 1) cancer cells undergo epithelial-mesenchymal transition (EMT). Subsequent studies have manifested that zinc finger E-box-binding homeobox 1 (ZEB1), an activation factor that promotes EMT, can enable cancer cells to gain stemness[16]. 2) Cancer cells under the hypoxic express a large number of hypoxia-inducible factor1-alpha (HIF-1α) and HIF-2α. HIF-1α can strengthen the activity of Notch pathway, down-regulate the activity of the DNA mismatch repair (MMR) system and increase the instability of genomes. HIF-2α can regulate the expressions of OCT4 and SOX2 genes, thereby promoting the common cancer cells in the hypoxic area to obtain stemness so as to transform into CSCs[17,18]. 3) Gene stability of cancer cells decline due to external factors. Liang et al[12] processed nasopharyngeal carcinoma and neuroblastoma cells with ultraviolet radiation or mitomycin *in-vitro* experiments, and they ascertained that cancer cells obtain stem cell properties while the instability of cancer cell genomes is on the rise, thus increasing the number of side populations and CD133$^+$ cells. The specific mechanism of radiation-induced cancer cell stemness will be further studied in future.

Based on previous experimental work and screening, 4 Gy X-ray radiation was applied in this study[19]. It was revealed that X-rays cause the transformation of cancer cells into CSCs, which provided new evidence showing that CSCs can be obtained from cancer cells and insert new insights for tumor metastasis, recurrence, radiation resistance and other problems in the current treatment of tumors. However, there were also deficiencies in the experiment: 1) a small amount of CD133$^+$ cells still remained in the CD133$^-$ cell group that was sorted by magnetic beads. 2) Ray radiation at only one dose was used. In subsequent studies, the effects of X-ray radiation at different doses on cancer cells will be explored. 3) The experimental results indicated that the enhanced stemness in the CD133$^-$ cell group was related to the up-regulated expressions of OCT4, SOX2, and Nanog genes, but the specific mechanism remains to be further studied.

Conclusions

We found that X-ray radiation at LD50 can enhance the stemness potential by up-regulating the expression of stemness-related genes in nasopharyngeal carcinoma CD133$^-$ cells.

Acknowledgements

National Natural Science Foundation of China (81501520); Natural Science Foundation Project of CQ (cstc2014jcyjA10021, cstc2015jcyjA10021).

Conflict of Interest

The authors declared no conflict of interest.

References

1) Charafe-Jauffret E, Ginestier C, Bertucci F, Cabaud O, Wicinski J, Finetti P, Josselin E, Adelaide J, Nguyen TT, Monville F, Jacquemier J, Thomassin-Piana J, Pinna G, Jalaguier A, Lambaudie E, Houvenaeghel G, Xerri L, Harel-Bellan A, Chaffanet M, Viens P, Birnbaum D. ALDH1-positive cancer stem cells predict engraftment of primary breast tumors and are governed by a common stem cell program. Cancer Res 2013; 73: 7290-7300.
2) Liu H, Wang YJ, Bian L, Fang ZH, Zhang QY, Cheng JX. CD44+/CD24+ cervical cancer cells resist radiotherapy and exhibit properties of cancer stem cells. Eur Rev Med Pharmacol Sci 2016; 20: 1745-1754.
3) Nishi M, Akutsu H, Kudoh A, Kimura H, Yamamoto N, Umezawa A, Lee SW, Ryo A. Induced cancer stem-like cells as a model for biological screening and discovery of agents targeting phenotypic traits of cancer stem cell. Oncotarget 2014; 5: 8665-8680.
4) Kharfan-Dabaja MA, Anasetti C, Santos ES. Hematopoietic cell transplantation for chronic lymphocytic leukemia: an evolving concept. Biol Blood Marrow Transplant 2007; 13: 373-385.
5) Moreno R, Rojas LA, Villellas FV, Soriano VC, Garcia-Castro J, Fajardo CA, Alemany R. Human menstrual blood-derived mesenchymal stem cells as potential cell carriers for oncolytic adenovirus. Stem Cells Int 2017; 2017: 3615729.
6) Nair N, Calle AS, Zahra MH, Prieto-Vila M, Oo A, Hurley L, Vaidyanath A, Seno A, Masuda J, Iwasaki Y, Tanaka H, Kasai T, Seno M. A cancer stem cell model as the point of origin of cancer-associated fibroblasts in tumor microenvironment. Sci Rep 2017; 7: 6838.
7) Zhuang HW, Mo TT, Hou WJ, Xiong GX, Zhu XL, Fu QL, Wen WP. Biological characteristics of CD133(+) cells in nasopharyngeal carcinoma. Oncol Rep 2013; 30: 57-63.
8) Meyer S, Worsdorfer P, Gunther K, Thier M, Edenhofer F. Derivation of adult human fibroblasts and their direct conversion into expandable neural progenitor cells. J Vis Exp 2015: e52831.
9) Do DV, Ueda J, Messerschmidt DM, Lorthongpanich C, Zhou Y, Feng B, Guo G, Lin PJ, Hossain MZ, Zhang W, Moh A, Wu Q, Robson P, Ng HH, Poellinger L, Knowles BB, Solter D, Fu XY. A genetic and developmental pathway from STAT3 to the OCT4-NANOG circuit is essential for maintenance of ICM lineages in vivo. Genes Dev 2013; 27: 1378-1390.
10) Su YJ, Lin WH, Chang YW, Wei KC, Liang CL, Chen SC, Lee JL. Polarized cell migration induces cancer type-specific CD133/integrin/Src/Akt/GSK3beta/beta-catenin signaling required for maintenance of cancer stem cell properties. Oncotarget 2015; 6: 38029-38045.
11) Koren E, Fuchs Y. The bad seed: cancer stem cells in tumor development and resistance. Drug Resist Updat 2016; 28: 1-12.
12) Lee SH, Hong HS, Liu ZX, Kim RH, Kang MK, Park NH, Shin KH. TNFalpha enhances cancer stem cell-like phenotype via Notch-Hes1 activation in oral squamous cell carcinoma cells. Biochem Biophys Res Commun 2012; 424: 58-64.
13) Liang Y, Feng Q, Hong J, Feng F, Sang Y, Hu W, Xu M, Peng R, Kang T, Bei J, Zeng Y. Tumor growth and metastasis can be inhibited by maintaining genomic stability in cancer cells. Front Med 2015; 9: 57-62.
14) Bao S, Wu Q, McLendon RE, Hao Y, Shi Q, Hjelmeland AB, Dewhirst MW, Bigner DD, Rich JN. Glioma stem cells promote radioresistance by preferential activation of the DNA damage response. Nature 2006; 444: 756-760.
15) Chihak MA, Ahmed SK, Lachance DH, Nageswara RA, Laack NN. Patterns of failure and optimal radiotherapy target volumes in primary intradural extramedullary Ewing sarcoma. Acta Oncol 2016; 55: 1057-1061.
16) Liu S, Cong Y, Wang D, Sun Y, Deng L, Liu Y, Martin-Trevino R, Shang L, McDermott SP, Landis MD, Hong S, Adams A, D'Angelo R, Ginestier C, Charafe-Jauffret E, Clouthier SG, Birnbaum D, Wong ST, Zhan M, Chang JC, Wicha MS. Breast cancer stem cells transition between epithelial and mesenchymal states reflective of their normal counterparts. Stem Cell Rep 2014; 2: 78-91.
17) Al TZ, Petry A, Chi TF, Mennerich D, Gorlach A, Dimova EY, Kietzmann T. Differential transcriptional regulation of hypoxia-inducible factor-1alpha by arsenite under normoxia and hypoxia: involvement of Nrf2. J Mol Med (Berl) 2016; 94: 1153-1166.
18) Toledo RA. New HIF2alpha inhibitors: potential implications as therapeutics for advanced pheochromocytomas and paragangliomas. Endocr Relat Cancer 2017; 24: C9-C19.
19) Wang W, Hou X, Yan J, Shen J, Lian X, Sun S, Liu Z, Meng Q, Wang D, Zhao M, Qiu J, Hu K, Zhang F. Outcome and toxicity of radical radiotherapy or concurrent Chemoradiotherapy for elderly cervical cancer women. BMC Cancer 2017; 17: 510.